Research Article • DOI: 10.2478/s13380-013-0129-y • Translational Neuroscience • 4(3) • 2013 • 363-367

VERSITA

ANATOMICAL LOCATION OF TRANSCALLOSAL SENSORIMOTOR FIBERS IN THE HUMAN BRAIN: DIFFUSION TENSOR TRACTOGRAPHY STUDY

Jung Pyo Seo,
Sung Ho Jang*

Department of Physical Medicine and Rehabilitation, College of Medicine, Yeungnam University

Abstract

Many diffusion tensor tractography (DTT) studies have reported on the topography of transcallosal fibers (TCF). However, little detailed anatomical information on TCF that can be easily applied for clinical purposes is known. Using probabilistic DTT, we attempted to determine the anatomical location of the TCF for motor and sensory function in the human brain. A total of 51 healthy subjects were recruited for this study. Diffusion tensor images (DTIs) were obtained at 1.5 T, and four TCF for the premotor cortex (PMC), the primary motor cortex (M1) for hand and leg, and the primary somatosensory cortex (S1) were obtained using FMRIB software. Locations of the TCF were defined as the highest probabilistic location on the midsagittal slice of the corpus callosum. We measured distances between the most anterior and posterior points of the corpus callosum. The relative mean distances of the highest probabilistic location for the precentral knob PMC (Brodmann area 6 anterior to the precentral knob), hand M1, leg M1, and precentral knob S1 (postcentral gyrus posterior to the precentral knob) TCF were 48.99%, 59.78%, 67.93%, and 73,48% from the most anterior point of the CC, respectively. According to our findings, the precentral knob PMC, hand M1, leg M1, and precentral knob S1 TCF were located at the anterior body, posterior body, posterior body, and isthmus according to Witelson's classification, respectively.

Keywords

• Corpus callosum • Diffusion tensor imaging • Transcallosal fiber • Motor function

Received 10 July 2013
accepted 30 July 2013

Introduction

The corpus callosum (CC) is the largest white matter fiber bundle connecting the two hemispheres of the brain [1,2]. Therefore, injury of the CC can result in various and severe manifestations depending on the location of the lesion, such as callosal disconnection syndrome (CDS), which is characterized by impairment of interhemispheric transfer of information due to interruption of transcallosal fibers (TCF) [3-6]. In addition, the CC has been a target structure for surgery to control seizure and for tumor resection [7]. Therefore, exact anatomical information on TCF, which are related to cerebral function, could be important to neuroscience clinicians.

In the past, because conventional brain CT and MRI cannot visualize the connection of the hemispheres by the TCF, assessment of TCF has been difficult. By contrast, recent advancements in diffusion tensor tractography (DTT), derived from DTI, have now allowed visualization of the architecture and integrity of TCF in three dimensions [8-11]. Many DTT studies have reported on the topography of TCF [12-21]. However, little is known about detailed anatomical information on TCF that can be easily applied for clinical purposes [14,15,22]. In the current study, using DTT, we attempted to determine the anatomical location of the TCF for motor and sensory function in the human brain.

Subjects and Methods

Subjects

A total of 51 healthy, right-handed subjects (31 men, 20 women; mean age 33.10 ± 8.26 years; range 20~49 years) with no previous history of neurological, psychiatric, or physical illness were recruited for this study. All subjects understood the purpose of the study, and provided written, informed consent prior to participation. The study protocol was approved by our Institutional Review Board.

Data acquisition

DTIs were acquired using a sensitivity-encoding head coil on a 1.5 T Philips Gyroscan Intera unit (Hoffman-La Roche, Best, The Netherlands) by single-shot echo-planar imaging using a navigator echo. For each of the 32 non-collinear diffusion sensitizing gradients, we acquired 60 contiguous slices parallel to the anterior commissure-posterior commissure line. Imaging parameters were as follows: acquisition matrix = 96×96, reconstructed to matrix = 128 × 128 matrix, field of view = 221 × 221 mm^2, TR = 10,726 ms, TE = 76 ms, SENSE factor = 2, EPI factor = 67 and b = 1000 s/mm^2, NEX = 1, slice gap = 0 mm, and slice thickness = 2.3 mm.

Fiber tracking

The Oxford Centre for Functional Magnetic Resonance Imaging of the Brain (FMRIB) Software Library software (FSL; www.fmrib.ox.ac.uk/fsl) was used for analysis of diffusion-weighted imaging data. Head motion effect and image distortion due to eddy currents were corrected by affine multi-scale two-dimensional registration. In this study, a probabilistic tractography method based on a multifiber model was used in performance

* *E-mail: strokerehab@hanmail.net*

of fiber tracking, and was applied by utilizing tractography routines implemented in FMRIB Diffusion (5000 streamline samples, 0.5 mm step lengths, curvature thresholds = 0.2) [23-25]. TCF were identified by selection of fibers passing through both regions of interest (ROIs). Seed ROIs were placed at both hemispheres, as follows; 1) the hand primary motor cortex (M1) TCF– precentral knob, 2) the leg M1 TCF – leg somatotopy of M1, 3) the precentral knob PMC TCF – anterior boundary: anterior margin of Brodmann area 6, posterior boundary: precentral sulcus, medial and lateral boundary: identical longitudinal lines with medial and lateral margin of the precentral knob, and 4) the precentral knob S1 TCF– anterior boundary: central sulcus, posterior boundary: postcentral sulcus, medial and lateral boundary: identical longitudinal lines with medial and lateral margin of the precentral knob [26] (Figure 1). A target ROI was given at the CC on the color map (red portion of midsagittal slice).

Determination of TCF location on CC

The locations of TCF were defined as the highest probabilistic location on the midsagittal slice of the CC in the anteroposterior direction. As shown in Figure 1, line a (the most anterior point of the CC) and line b (the most posterior point of the CC) were indicated in the CC, respectively. We measured the distance between line a and line b, and then between line a and the anterior margin of the highest probability point of each of the four TCF. Locations were calculated in pixel units. The locations of TCF were measured at the CC using the following equation:

$$\text{Antero-posterior distance (\%)} = \frac{\text{Distance between line a and highest probability point}}{\text{Distance between line a and line b}} \times 100$$

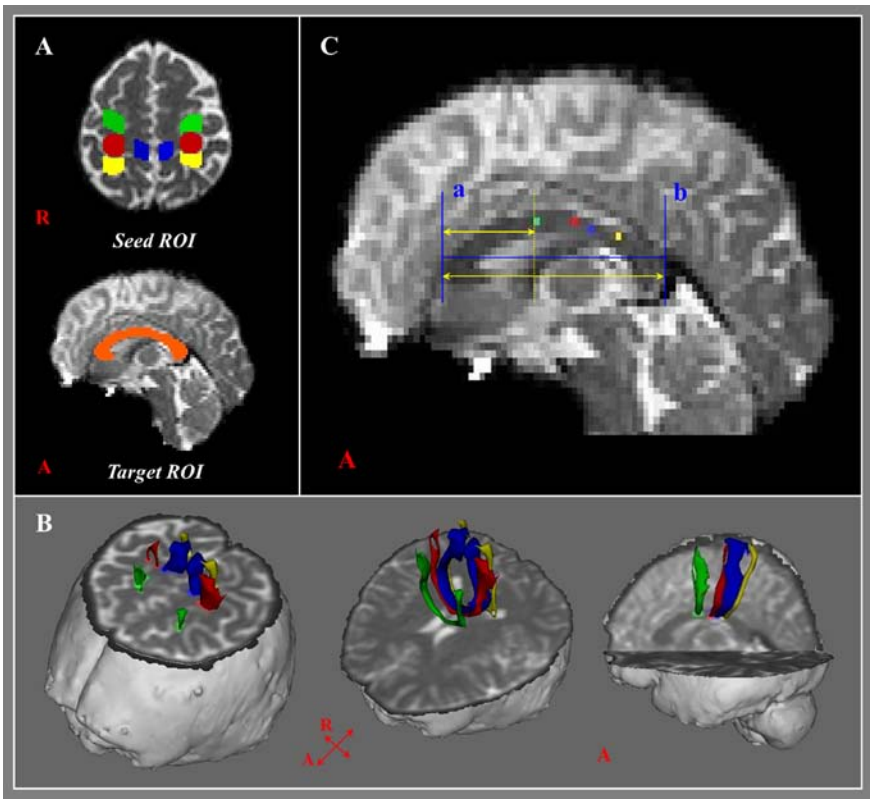

Figure 1. (A) Seed regions of interest (ROIs) were placed on the premotor cortex (PMC) of both hemispheres for the PMC transcallosal fibers (TCF) (green color), the precentral knobs of both hemispheres for the primary motor cortex (M1) TCF (red color), the leg somatotopies of both hemispheres for the leg TCF (blue color), and the primary somatosensory cortices (S1) of both hemispheres for the S1 TCF (yellow color). The target ROI was placed on the corpus callosum at the midsagittal slice (right). (B) TCF were reconstructed in both hemispheres. (C) Landmarks used to determine location of TCF (line a – passing through the anterior most point of the corpus callosum, line b – passing through the most posterior point of the corpus callosum).

Statistical analysis

SPSS software (v.15.0; SPSS, Chicago, IL) was used for data analysis. One-way ANOVA with LSD post-hoc test was used for determination of variances between the precentral knob PMC TCF, hand M1, leg M1, and precentral knob S1 TCF on the CC. Statistical significance was set at $p < 0.05$.

Results

The Leg M1 TCF were reconstructed in all 51 subjects. However, the hand M1 TCF were reconstructed in 41 (80.0%) of 51 subjects, and the precentral knob PMC and precentral knob S1 TCF were reconstructed in 36 (70.6%) of 51 subjects. Considering all of the results, all four TCF were reconstructed in 32 (62.7%) of 51 subjects.

We performed data analysis for the 32 subjects in whom all four TCF were reconstructed. A summary of the mean distances of the highest probabilistic locations for each TCF in the CC is shown in Table 1. The relative mean distances of the highest probabilistic location for the precentral knob PMC, hand M1, leg M1, and precentral knob S1 TCF were 48.99%, 59.78%, 67.93%, and 73.48% from the most anterior point of the CC, respectively. We observed significant differences between the highest probabilistic locations between the four TCF ($p < 0.05$).

Discussion

Before introduction of DTI, Witelson's classification was the general standard with regard to the topography of the CC in the human brain [27]. In 1989, Witelson conducted a postmortem morphological study of 50 consecutive human brains. He classified the CC into seven subdivisions, as follows: region 1: rostrum, region 2: genu, region 3: rostral body, region 4: anterior midbody, region 5: posterior midbody, region 6: isthmus, and region 7: splenium. Based primarily on experimental work with monkeys and some human clinical work, he suggested rough topography of TCF in relation to cortical regions, as follows: Witelson's classification 1, 2, 3 (anterior third); prefrontal, premotor, and supplementary

Table 1. Relative average distances of the highest probability points of transcallosal fibers in the midsagittal corpus callosum.

	Precentral knob PMC TCF	Hand M1 TCF	Leg M1 TCF	Precentral knob S1 TCF
Anterior to posterior distance (%)	48.99 (±5.45)	59.78 (±4.91)	67.93 (±3.15)	73.48 (±6.43)
	*	0.00	§	0.00
p – values	†	0.00	//	0.00
	‡	0.00	¶	0.00

Values indicate means (±standard deviations); M1: primary motor cortex; S1: primary somatosensory cortex; PMC: premotor cortex; TCF: transcallosal fibers.
Post-hoc LSD test was used for comparisons of diffusion tensor image parameters;
*: in precentral knob PMC TCF and hand M1 TCF.
†: in precentral knob PMC TCF and leg M1 TCF.
‡: in precentral knob PMC TCF and precentral knob S1 TCF.
§: in hand M1 TCF and leg M1 TCF.
//: in hand M1 TCF and precentral knob S1 TCF.
¶: in leg M1 TCF and precentral knob S1 TCF.

motor, Witelson's classification 4 (anterior midbody, anterior one-half minus anterior one-third); motor, Witelson's classification 5 (posterior midbody, posterior half minus the posterior third) somesthetic and posterior parietal, Witelson's classification 6 (isthmus, the posterior one-third minus the posterior one-fifth); posterior parietal and superior temporal, and Witelson's classification 7 (splenium, the posterior one-fifth); occipital and inferior temporal.

Since introduction of DTI, many studies have demonstrated topography of the TCF, which were located in a more posterior direction than those of Witelson's classification and previous monkey studies [13-16,20,22]. In 2006, using probabilistic DTT in 11 normal subjects, Zarei et al., reported that the premotor TCF were located in the mid-body region and the M1 TCF were located posterior to the premotor region, followed by the S1 tract [14]. They also reported the Talairach coordinates with maximal connectivity probability of the TCF. During the same year, using Witelson's classification, Hofer and Frahm suggested a different scheme based on DTTs of eight normal subjects: the premotor and supplementary motor (anterior half minus anterior one sixth); motor (posterior half minus the posterior third); and sensory (the posterior one-third minus posterior one-fourth) [13]. In 2007, Wahl et al. reported that transcallosal motor fibers crossed through the posterior body and isthmus, and the hand and foot transcallosal motor fibers were located in an anterior-posterior direction in 12 normal subjects [15]. Subsequently, by combining cortical gray matter parcellation with the DTT of 22 normal subjects, Park et al. [2008] reported that TCF from the sensorimotor cortex passed through the isthmus [16]. In 2010, in a study combining fMRI and DTT in 36 normal subjects, Salvolini et al. demonstrated that the TCF for motor task lay in the central portion of the body, and those for tactile stimulation were located in the posterior part of the body [20]. Recently, Fling et al. reported Talairach coordinates of five TCF for motor sensory function (pre-supplementary motor area, supplementary motor area, dorsal PMC, M1, and S1) in the sagittal CC in 21 normal subjects [22].

According to results of our study, the relative mean distances of the highest probabilistic locations for the precentral knob PMC, hand M1, leg M1, and precentral knob S1 TCF were 48.99%, 59.78%, 67.93%, and 73.48% between the most anterior point of the CC and the most posterior point of the CC, respectively. Considering Witelson's classification [27], our results corresponded to Witelson's subdivisions, as follows: the precentral knob PMC (anterior midbody), hand M1 (posterior midbody), leg M1 (posterior midbody), and precentral knob S1 TCF (isthmus). These results generally coincide with or are similar to results of previous DTI studies [13-16,20]. Three previous DTI studies reported Talairach coordinate data of TCF topography [14,15,22], however, it is not easy to apply such data in clinical practice. Here, however, we reported topography data on TCF that can be easily applied in the clinical field and based on a larger number of subjects compared with previous studies, as it was reported that the topography of the CC shows wide individual variation [2].

In conclusion, we investigated the anatomical locations of the TCF for motor sensory function; according to our findings, the relative mean distances of the highest probabilistic locations precentral knob PMC, hand M1, leg M1, and precentral knob S1 TCF were 48.99% (anterior body), 59.78% (posterior body), 67.93% (posterior body), and 73.48% (isthmus) between the most anterior and posterior points of the CC. We believe that these results will be helpful to neuroscience clinicians in clinical practice. However, the limitations of DTI should be considered. DTT is a powerful anatomic imaging tool for demonstration of gross fiber architecture; however, due to partial volume effect and fiber crossing, it has significant limitation in reconstruction of neural tracts [13,28-30]. In this study, although the leg M1 TCF were reconstructed in all 51 subjects, the precentral knob PMC and precentral knob S1 TCF were reconstructed in only 36 (70.6%) of 51 subjects. Therefore, we think that, in order to overcome this limitation, conduct of further studies would be necessary. On the other hand, clinical correlation studies are also encouraged.

Acknowledgement

This research was supported by Basic Science Research Program through the National Research Foundation of Korea (NRF) funded by the Ministry of Education, Science and Technology (2012R1A1A4A01001873). The authors have no conflict of interest to declare. Both authors had full access to all the data in the study and take responsibility for the integrity of the data and the accuracy of the data analysis.

References

[1] Jones E.G., Epilepsy and the corpus callosum, Plenum Press, New York, 1985
[2] Wahl M., Ziemann U., The human motor corpus callosum, Rev. Neurosci., 2008, 19, 451-466
[3] Watson R.T., Heilman K.M., Callosal apraxia, Brain, 1983, 106, 391-403
[4] Bogousslavsky J., Caplan L.R., Stroke syndromes, Cambridge University Press, Cambridge, 2001
[5] Bourekas E.C., Varakis K., Bruns D., Christoforidis G.A., Baujan M., Slone H.W., et al., Lesions of the corpus callosum: MR imaging and differential considerations in adults and children, AJR Am. J. Roentgenol., 2002, 179, 251-257
[6] Jea A., Vachhrajani S., Widjaja E., Nilsson D., Raybaud C., Shroff M., et al., Corpus callosotomy in children and the disconnection syndromes: a review, Childs Nerv. Syst., 2008, 24, 685-692
[7] Blume W.T., Corpus callosum section for seizure control: rationale and review of experimental and clinical data, Cleve. Clin. Q., 1984, 51, 319-332
[8] Molko N., Cohen L., Mangin J.F., Chochon F., Lehericy S., Le Bihan D., et al., Visualizing the neural bases of a disconnection syndrome with diffusion tensor imaging, J. Cogn. Neurosci., 2002, 14, 629-636
[9] Le T.H., Mukherjee P., Henry R.G., Berman J.I., Ware M., Manley G.T., Diffusion tensor imaging with three-dimensional fiber tractography of traumatic axonal shearing injury: an imaging correlate for the posterior callosal "disconnection" syndrome: case report, Neurosurgery, 2005, 56, 189
[10] Lin F., Yu C., Liu Y., Li K., Lei H., Diffusion tensor group tractography of the corpus callosum in clinically isolated syndrome, AJNR Am. J. Neuroradiol., 2011, 32, 92-98
[11] Chang M.C., Yeo S.S., Jang S.H., Callosal disconnection syndrome in a patient with corpus callosum hemorrhage: a diffusion tensor tractography study, Arch. Neurol., 2012, 69: 1374-1375
[12] Abe O., Masutani Y., Aoki S., Yamasue H., Yamada H., Kasai K., et al., Topography of the human corpus callosum using diffusion tensor tractography, J. Comput. Assist. Tomogr., 2004, 28, 533-539
[13] Hofer S., Frahm J., Topography of the human corpus callosum revisited -comprehensive fiber tractography using diffusion tensor magnetic resonance imaging, Neuroimage, 2006, 32, 989-994
[14] Zarei M., Johansen-Berg H., Smith S., Ciccarelli O., Thompson A.J., Matthews P.M., Functional anatomy of interhemispheric cortical connections in the human brain, J. Anat., 2006, 209, 311-320
[15] Wahl M., Lauterbach-Soon B., Hattingen E., Jung P., Singer O., Volz S., et al., Human motor corpus callosum: topography, somatotopy, and link between microstructure and function, J. Neurosci., 2007, 27, 12132-12138
[16] Park H.J., Kim J.J., Lee S.K., Seok J.H., Chun J., Kim D.I., et al., Corpus callosal connection mapping using cortical gray matter parcellation and DT-MRI, Hum. Brain Mapp., 2008, 29, 503-516
[17] Chao Y.P., Cho K.H., Yeh C.H., Chou K.H., Chen J.H., Lin C.P., Probabilistic topography of human corpus callosum using cytoarchitectural parcellation and high angular resolution diffusion imaging tractography, Hum. Brain Mapp., 2009, 30, 3172-3187
[18] Koerte I., Heinen F., Fuchs T., Laubender R.P., Pomschar A., Stahl R., et al., Anisotropy of callosal motor fibers in combination with transcranial magnetic stimulation in the course of motor development, Invest. Radiol., 2009, 44, 279-284
[19] Salvolini U., Polonara G., Mascioli G., Fabri M., Manzoni T., Functional topography of the human corpus callosum, Bull. Acad. Natl. Med., 2010, 194, 617-631; discussion 631-632
[20] Fabri M., Polonara G., Mascioli G., Salvolini U., Manzoni T., Topographical organization of human corpus callosum: an fMRI mapping study, Brain Res., 2011, 1370, 99-111
[21] Gawryluk J.R., D'Arcy R.C., Mazerolle E.L., Brewer K.D., Beyea S.D., Functional mapping in the corpus callosum: a 4T fMRI study of white matter, Neuroimage, 2011, 54, 10-15
[22] Fling B.W., Benson B.L., Seidler R.D., Transcallosal sensorimotor fiber tract structure-function relationships, Hum. Brain Mapp., 2013, 34, 384-395
[23] Behrens T.E., Johansen-Berg H., Woolrich M.W., Smith S.M., Wheeler-Kingshott C.A., Boulby P.A., et al., Non-invasive mapping of connections between human thalamus and cortex using diffusion imaging, Nat. Neurosci., 2003, 6, 750-757
[24] Smith S.M., Jenkinson M., Woolrich M.W., Beckmann C.F., Behrens T.E., Johansen-Berg H., et al., Advances in functional and structural MR image analysis and implementation as FSL, Neuroimage, 2004, 23 Suppl. 1, S208-219
[25] Behrens T.E., Berg H.J., Jbabdi S., Rushworth M.F., Woolrich M.W., Probabilistic diffusion tractography with multiple fibre orientations: What can we gain?, Neuroimage, 2007, 34, 144-155
[26] Hong J.H., Son S.M., Jang S.H., Somatotopic location of corticospinal tract at pons in human brain: a diffusion tensor tractography study, Neuroimage, 2010, 51, 952-955
[27] Witelson S.F., Hand and sex differences in the isthmus and genu of the human corpus callosum. A postmortem morphological study, Brain, 1989, 112, 799-835
[28] Wiegell M.R., Larsson H.B., Wedeen V.J., Fiber crossing in human brain depicted with diffusion tensor MR imaging, Radiology, 2000, 217, 897-903

[29] Parker G.J., Alexander D.C., Probabilistic anatomical connectivity derived from the microscopic persistent angular structure of cerebral tissue, Philos. Trans. R. Soc. Lond. B Biol. Sci., 2005, 360, 893-902

[30] Yamada K., Sakai K., Akazawa K., Yuen S., Nishimura T., MR tractography: a review of its clinical applications, Magn. Reson. Med. Sci., 2009, 8, 165-174